

# HEAT TRANSFER AT SUPERCRITICAL STATE FOR ORGANIC RANKINE APPLICATIONS

**Marija LAZOVA<sup>(\*)</sup>, Alihan KAYA<sup>(\*)</sup>, Henk HUISSEUNE<sup>(\*)</sup> Michel DE PAEPE<sup>(\*)</sup>**

<sup>(\*)</sup> Ghent University, Sint-Pietersnieuwstraat 41, Ghent, 9000, Belgium  
Marija.Lazova@Ugent.be

## ABSTRACT

In the last years, a lot of attention has been paid for developing technologies for low grade heat recovery. This work focuses on the possibilities to increase the performance of the Organic Rankine Cycle, by utilizing low grade heat source within a temperature range of 90°C - 200°C.

One way to improve the performance is a proper selection and design of the components. On the other hand, a way of enhancing the overall cycle efficiency is introduced with supercritical heat transfer in the heat exchanger. The advantage is a better thermal match between the heat source and the working fluid temperature profiles in the heat exchanger. Because, correlations available from literature were used for designing of this component safety factor was also implemented to reduce the uncertainty level.

In this work, results from measurement campaigns for a heat exchanger obtained at supercritical state are presented. It can be concluded that improving the design of the heat exchanger leads to better cycle efficiency and reducing the cost of an ORC installation.

## 1. INTRODUCTION

Organic Rankine Cycles (ORC) are considered as suitable technology for converting low-grade heat sources (e.g. from process industry, solar energy, etc.) to usable electrical energy. Even though this technology is not new and is well developed, there is still room for improvement of the performance and the efficiency of these cycles. In order to have good performance of the cycle, a proper design and selection of the components have to be done. On the other hand, a way of enhancing the overall cycle efficiency in ORC is introduced with supercritical heat transfer in the heat exchanger.

As main challenge to work with supercritical ORCs, is a better thermal match temperature profiles between the heat source and the working (organic) fluid in the heat exchanger. Moreover, at supercritical state there are strong variations of the thermophysical properties of the fluid. As the value of the heat transfer coefficient depends on these variations, it is important to study and understand the behaviour of the fluid properties when going from subcritical to supercritical state. In order to have a proper design of heat exchanger suitable to work at supercritical conditions it is important to determine the local heat transfer coefficients and correlations.

Other important parameters that influence on the heat transfer are the working fluid flow direction, tube diameter, heat and mass flux, buoyancy and selection of proper organic fluid.

In the past years, more precisely starting from 1950s [1], [2], [3] a lot of research activities regarding supercritical heat transfer have been performed. Tests had been done mainly in vertical positioning with various tubes diameters [4], [5], [6]. There are also many paper related to heat transfer in critical and near-critical region for variety of working fluids such as water, carbon dioxide and helium [7], [8]. This necessitates development of new correlations suitable for supercritical working conditions for ORCs and fluids of interests. Therefore, in order to provide useful correlations for design of a heat exchanger the heat transfer process to the working fluids at supercritical conditions has to be studied [9].

Even though the research activities regarding supercritical heat transfer started long time ago the first published paper found in the literature regarding supercritical ORC dates from 1981[10]. Haskins (1981) performed research activities of solar receiver coupled to a supercritical ORC engine in order to maximize the thermal efficiency by using toluene as working fluid.

A basic layout of a supercritical ORC is presented in Figure 1. The cycle components are a supercritical pump, a vapour generator (heat exchanger), an expander and a condenser. The working fluid is pumped

above its critical pressure (from state point 1 until state point 2) and then heated with a constant supercritical pressure from liquid directly to supercritical vapour (state point 3). The supercritical vapour is expanded in the expander (turbine) to extract mechanical work (from state point 3 until state point 4). After expansion, the fluid is condensed in the condenser by dissipating heat to a heat sink (state point 4 until state point 1) and the condensed liquid is then pumped to the high pressure again, which completes the cycle. In an actual cycle there will be some pressure loss in the vapour generator (2-3) and condenser (4-1). Furthermore, there is no big difference on component level between the subcritical and supercritical cycles. In supercritical cycles the heat exchanger instead of evaporator is named vapour generator because the two-phase region is omitted and evaporation is no longer occurring.

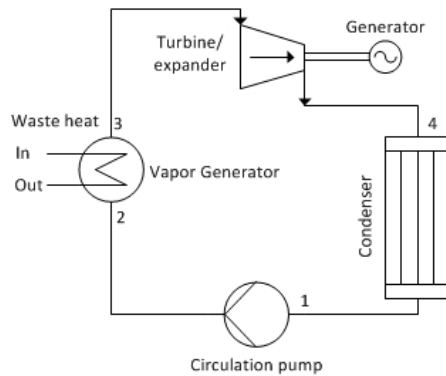


Figure 1. Schematic overview of supercritical ORC

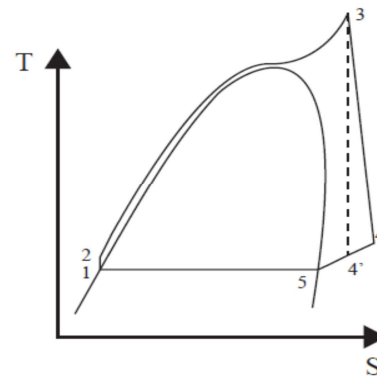


Figure 2. T,s-diagram of supercritical cycle

Figure 2 presents T,s - diagram of a supercritical cycle, where it can be noticed that the working fluid from liquid-like region before expansion is heated to a gas-like phase while omitting the two phase heat addition. Furthermore, from the literature review [11] it had been concluded that there is lack of knowledge of the heat transfer to the applied working (organic) fluids within these supercritical ORCs. The main reason is the difference of the working conditions of an ORC plant such as relatively higher temperature and pressure. This lack of knowledge necessitates the development of new heat transfer correlation for working fluids used under the supercritical conditions in ORC. An inaccurate correlations lead to an over-sizing of heat exchangers, thus resulting in a lower economic feasibility of such cycles. The heat exchanger represents key component in every ORC engine. This component dictates the efficiency of the cycle and the total cost of one ORC plant. It is estimated that the cost of the heat exchanger is usually up to 30% of the total cost of an ORC where evaporator, (regenerator) and condenser are taken into account [12]. Because the ratio of the total heat exchanger area to net power output in an ORC is considerably high it presents an important issue of consideration.

Hence, from the arguments mentioned above it can be concluded that more accurate design of the heat exchanger with appropriate correlations leads to improved cycle efficiency and lowering the cost of such installation. In this work a supercritical heat exchanger is designed and constructed using literature correlations. Next, the heat exchanger is tested and the measurements are compared to the design specs.

## 2. SUPERCRITICAL HEAT EXCHANGER DESIGN

### 2.1. Design specifications

A helical coil heat exchanger is fabricated out of metal coil - tube that is fitted in annular portion of two concentric cylinders. The working fluid R404a flows in upward direction in the helical coil and the heat source (water-glycol) flows downward in the annulus resulting in a counter-flow configuration. The heat transfer takes place across the coil wall. The dimensions of both cylinders are determined by the velocity needed to meet heat transfer requirements. Figure 3 presents the configuration of the helical-coil heat exchanger.

A representative supercritical heating process is presented in Figure 4, showing the temperatures of the heat transfer fluid and an organic fluid R404a, with a pinch point temperature difference of 10 K, which exists at the organic fluid's outlet.

The selection of the heat exchanger is accomplished taking into account that the velocity and pressure drop in the tube and annulus are within the allowable ranges.

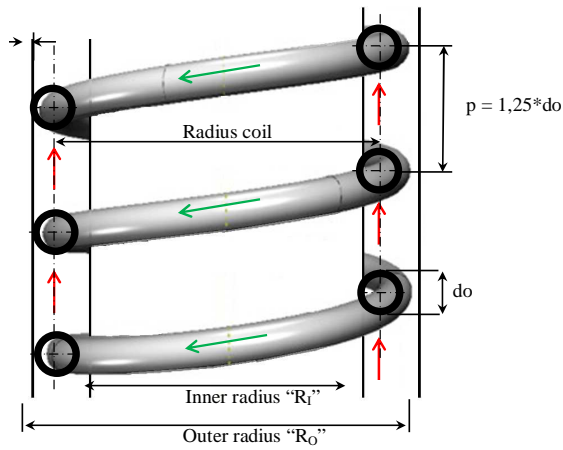


Figure 3. Schematic cut-away view of a helical-coil

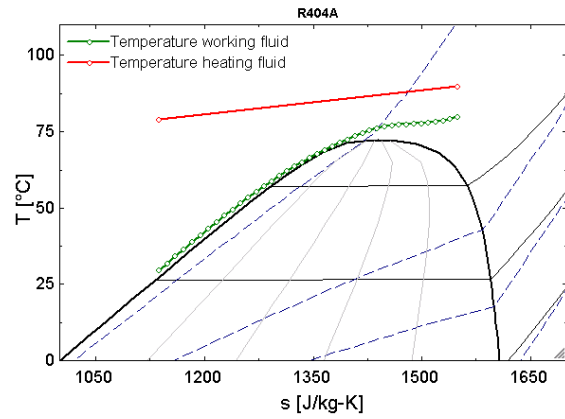


Figure 4. T,s-diagram of the heating process in the supercritical heat exchanger

The velocity ranges of the working fluid R404a were fixed at minimum 0,5 m/s and maximum 2,17 m/s, the overall pressure drop was neglected in the calculation and was afterwards calculated and should be lower than 40 kPa. The heating fluid is flowing relatively slow ( $Re = 4200 - 5900$ ).

## 2.2. Design methodology

A widely used method of calculating the heat transfer capacity (UA) and eventually sizing the heat exchanger is the logarithmic mean temperature difference (LMTD) method, applied between the inlet and outlet of the heat exchanger [13], [14], [15], and given by Eq. (1).

$$\dot{Q} = U \cdot A \cdot \Delta T_{log} = U \cdot A \cdot \frac{\Delta T_1 - \Delta T_2}{\ln\left(\frac{\Delta T_1}{\Delta T_2}\right)} \quad (1)$$

where  $Q$  is the heat transferred,  $U$  the overall heat transfer coefficient,  $A$  the total heat exchanging surface and  $\Delta T_{log}$  is the logarithmic temperature difference or LMTD. There is assuming that a generic heat exchanger (or a heat exchanging control volume) has two ends ('1' and '2') at which the hot and cold streams enter or exit on either side. However, the LMTD-method is based on constant fluid properties, an assumption leading to incorrect results in the case of supercritical fluids. An alternative solution consists in discretizing the heat exchangers to a large number of control volumes so that the properties variation in each step is small and an average constant value can be assigned within each volume. The discretization is performed in EES (Engineering Equation Solver) by dividing the overall enthalpy change for one of the streams in  $N$  (here  $N = 40$ ) equal differences  $dh$ . Discretization is advisable to be in the range between 20 and 40 equal distances. Lower than 20 leads to inaccurate results, while above 40 is not desirable due to there is no big difference in the terms of accuracy but is time consumable.

### 2.2.1. Heat transfer coefficient at the shell side (annulus)

In a helical-coil heat exchanger, the heating fluid is circulated in the annulus. As the flow rate of the heating fluid is rather low, the following Nusselt-correlation, valid for Reynolds number ( $Re$ ) between 50 and 10000 can be used (Eq. (8)) [16].

$$Nu = 0,6Re^{0,5}Pr^{0,31} \quad (2)$$

where  $Pr$  is the Prandtl number.

For higher Reynolds number ( $Re > 10000$ ), Eq. (9) is used [17].

$$Nu = 0,36Re^{0,55}Pr^{\frac{1}{3}}(\mu/\mu_w)^{0,14} \quad (3)$$

where  $\mu$  is the fluid's bulk viscosity and  $\mu_w$  is the fluid's viscosity at the wall temperature.

### 2.2.2. Heat transfer coefficient at the helical coil side

At the helical coil side supercritical fluid is circulated in upward flow. Several correlations can be found in the literature for the calculation of the heat transfer coefficient at supercritical conditions. In this work three

correlations for sizing of the heat exchanger are identified and compared. The conventional heat transfer correlations for single phase flow (calculation of the Nusselt number) cannot be used in the current case, due to the variations of the fluid properties around the critical point. For the calculations of the helical coil heat exchanger, three heat transfer correlations are compared.

Petukhov et al. [18] developed correlations for supercritical fluid parameters. The correlations have a correction factor, which neutralizes the effect of the variations of the thermo-physical properties around the pseudo-critical point and provides more stable and accurate results. The Nusselt-correlation proposed by Petukhov et al. [6] for carbon dioxide in the supercritical range at high temperature drops takes into account the difference in properties between the wall and the bulk, and is given below. This correlation was originally developed for carbon dioxide, but can be applied for the organic fluid R404a.

$$Nu_b = Nu_{0,b} \left( \frac{\bar{c}_p}{c_{p,b}} \right)^{0.35} \left( \frac{\lambda_b}{\lambda_w} \right)^{-0.33} \left( \frac{\mu_b}{\mu_w} \right)^{-0.11} \quad (4)$$

where  $b$  refers to the bulk fluid temperature and  $w$  to the wall temperature.

The heat-transfer coefficient of the organic fluid flowing inside the coil is calculated using the correlations for supercritical heat transfer in a straight pipe. This coefficient is then corrected for a coiled tube by multiplying it by a factor:  $F_{helical}$ , given by Schmidt's correlation, which has a large application range [19].

$$F_{helical} = 1 + 3,6 \left[ 1 - \frac{d_i}{D_H} \right] \left( \frac{d_i}{D_H} \right)^{0,8} \quad (5)$$

This expression is applicable for  $2 \times 10^4 < Re < 1.5 \times 10^5$  and for  $5 < R/a < 84$ , with  $R$  the radius of the coil [m] and  $a$  the radius of the tube [m].

The term  $Nu_{0,b}$  is calculated using the following Petukhov-Kirillov correlation [20] and the bulk temperature of the fluid.

$$Nu_{0,b} = \left( \frac{\frac{f_b Re_b \bar{Pr}}{8}}{12.7 \left( \frac{f_b}{8} \right)^{0.5} \left( \frac{2}{Pr^3} - 1 \right) + 1.07} \right) \quad (6)$$

where the Darcy friction factor ( $f$ ) is expressed as:

$$f = (1.82 \log_{10}(Re_b) - 1.64)^{-2} \quad (7)$$

The average specific heat  $\bar{c}_p$  is defined as:

$$\bar{c}_p = \frac{h_b - h_w}{T_b - T_w} \quad (8)$$

Garimella [21] developed correlations for supercritical heat transfer based on measurement data from refrigerants bends R410a and R404a. Three regions of heat transfer were identified based on the state of the heat transferring fluid: Liquid-like region, Pseudo-critical transition and Gas-like region. For each region a separate correlation for Nusselt number and friction factor was identified. However, these correlations were developed for smaller diameter (9,4 and 6,2 mm) and for supercritical heat transfer cooling applications. As already mentioned in the text the tube diameter has influence on the heat transfer rate. The designed supercritical heat exchanger has relatively higher inner diameter of 26 mm and the working conditions are different from one for ORC application. Therefore, these correlations were taken into account and compared to other without completely relying during the design process. The average uncertainties in these heat transfer coefficients were  $\pm 10\%$ . These correlations are listed in continuation;

Liquid-like region:

$$Nu = 1,421 Nu_{churchil-modified} (C_{p,w}/C_{p,b})^{0,444} (d_{actual}/d_{baseline})^{-0,183} \quad (15)$$

Pseudo-critical transition:

$$Nu = 1,350 Nu_{churchil-modified} (C_{p,w}/C_{p,b})^{0,249} (d_{actual}/d_{baseline})^{-0,066} \quad (16)$$

Gas-like region:

$$Nu = 1,556 Nu_{churchil-modified} (C_{p,w}/C_{p,b})^{-0,212} (d_{actual}/d_{baseline})^{-0,308} \quad (17)$$

These correlations are valid for the following working range:  $200 \text{ kg/m}^2\text{s} < G < 800 \text{ kg/m}^2\text{s}$  and  $1.0 < P/P_{cr} < 1.2$ . Also there are correction factors developed for all flow regimes boundaries [21].

The majority of empirical correlations were proposed in the 1960s – 1970s, when experimental techniques were not at the same level (i.e., advanced level) as they are today. Also, thermo-physical properties of water have been updated since that time (for example, a peak in thermal conductivity in critical and pseudo-critical points within a range of pressures from 22,1 to 25 MPa was not officially recognized until the 1990s). Therefore, recently a new or an updated correlation, based on a new set of heat-transfer data and the latest thermo-physical properties was developed and evaluated (Mokry et al. [22]):

$$Nu = 0,0061Re^{0,904}Pr^{0,684}(\rho_w/\rho_b)^{0,564} \quad (18)$$

This correlation is valid for the following working range:  $200 \text{ kg/m}^2\text{s} < G < 1500 \text{ kg/m}^2\text{s}$ .

### 2.3. Dimensions of the heat exchanger

As summary, the final design of the heat exchanger leads to coil length of 66 m and inner diameter of the coil of 26 mm. To account for heat transfer correlation uncertainty the heat exchanger is oversized by about 20%. Table 1 presents summary of the heat exchanger design.

Table 1. Summary of the heat exchanger design

Helical coil heat exchanger										
$d_o$	t	L	$D_i$	$D_o$	$D_c$	H	A	Q	$h_{hf\_avg}$	$h_{wf\_avg}$
[mm]	[mm]	[m]	[m]	[m]	[m]	[m]	[m <sup>2</sup> ]	[kW]	[W/m <sup>2</sup> K]	[W/m <sup>2</sup> K]
33.7	4	66	0.526	0.674	0.6	1.508	6.988	41	403	2200

where  $d_o$  is the tube outer diameter, t the tube thickness,  $D_i$  the inner shell diameter,  $D_o$  the outer shell diameter,  $D_c$  the coil diameter, H the height of the HX and A the total heat exchanger surface. Q is the heat transfer capacity of the heat exchanger coefficient.  $h_{avg}$  is the average heat transfer coefficient.

## 3. EXPERIMENTAL TEST SET-UP

The experimental test set-up consists of heat source installation and ORC system. Heat sources that can be utilized for these applications are waste heat recovery from industry processes, solar and geothermal energy sources and others. The temperature range that is of interest in this research work is between 90°C to 200°C. Figure 5 illustrates simplified layout of the experimental test set-up. During the experimental campaigns, temperature and pressure measurements were conducted. The positioning of the pressure and temperature sensors is indicated in Figure 3. In order to evaluate the performance, one temperature sensor is placed at the inlet and one at the outlet of the heat exchanger and the heat source respectively. It is important to be mentioned that the system is well insulated, which means that the heat loss to the environment is reduced. Several measurements campaigns were done, where the supercritical state was achieved under the following conditions presented and compared with the designing condition in Table 2;

Table 2 Summary of the design and measurement conditions

	MEASUREMENTS		DESIGN	
<b>m_wf</b>	2,7	[kg/s]	2,5	[kg/s]
<b>T_hf_in</b>	101	[°C]	95	[°C]
<b>m_wf</b>	0,226	[kg/s]	0,2539	[kg/s]
<b>T_wf</b>	36,3	[°C]	27,37	[°C]
<b>p_crit</b>	1,026		1,034	
<b>Q</b>	36	kW	41	kW

While running the measurements these values were held constant. As presented in the table the design and measurements conditions vary which gives lower heat transfer capacity. The difference between the initially designed model and the built component in the heat transferred and that is 41 kW and 36 kW respectively. The aim of these measurements was to evaluate the performance of the heat exchanger working at supercritical state. This component is first of its kind specially designed and build for an ORC installation, suitable to operate at relatively higher pressure and temperature.

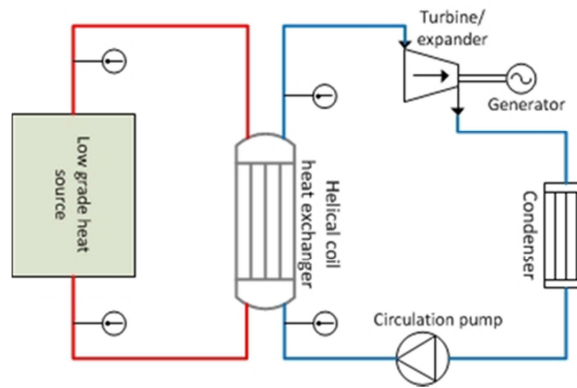


Figure 5. Layout of the experimental test set-up

## 4. COMPARISON BETWEEN RESULTS OBTAINED FROM THE DESIGN AND EXPERIMENTAL MEASUREMENTS OF THE SUPERCRITICAL HEAT EXCHANGER

### 4.1. Analysis of the design and measurement constraints of the heat exchanger

To check the performance of the helical coil heat exchanger, the influence of changing mass flow rate to the heat transferred and the outlet temperatures at cold and hot side is investigated. The constraints are presented in Table 2. The outlet temperatures at the cold and hot side and the pinch point temperature difference are determined by the flow rates and inlet temperatures.

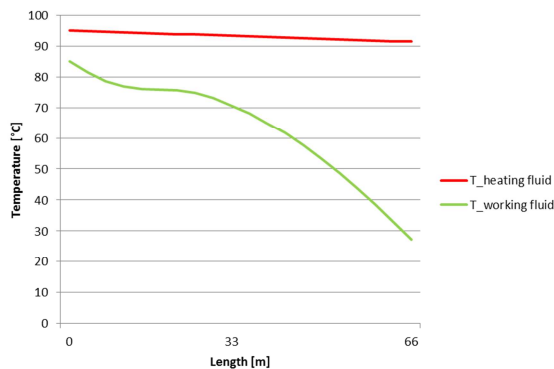


Figure 6. PP temperature difference off-design

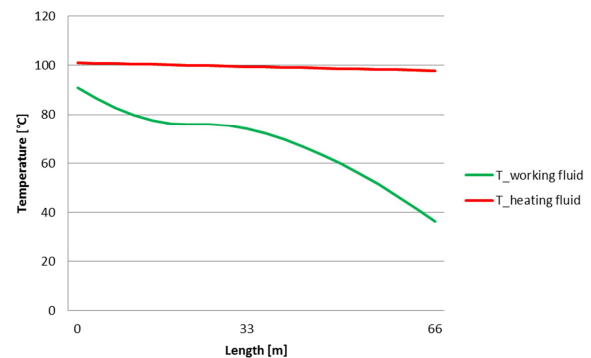


Figure 7. PP temperature difference measurements

By changing the flow rate of the heating fluid without changing the flow rate of the working fluid will result in a decrease of the outlet temperature of the heating fluid, a decrease of the outlet temperature of the working fluid and an increase of the pinch point temperature difference. The designed pinch point temperature difference is 10 K.

From the sets of measurements covering supercritical operation specific conclusions are reached about the heat exchanger performance. Namely, the main advantage is the very low temperature differences between the heating fluid and the organic fluid R404a (in the range of 1.5-2.5 °C). Moreover, the pressure drop of the heating fluid is very small and equal to 0.1-0.2 bar, while that of the organic fluid R404a is higher and in the range of 0.6-1 bar. This value is low, which should be however considered during the design stage, in order to select the correct size of this component.

In figure 6 and 7 the pinch point temperature difference (design and measurements) between the heating fluid and the working fluid R404a is presented.

### 4.2. Development of new correlation suitable for helical coil heat exchanger

Using a modified Wilson method [23], [24] the mean value of the convection coefficient outside the tubes and the convection coefficient inside the tubes as a function of the working fluid mass flow (or velocity) are obtained. Figure 8 is logarithmic graph that describes the Nu number as a function of the Re and Pr number. This graph presents comparison of the experimental data and the correlations used from literature. Moreover, the coefficient C and the exponent of the Reynolds number m of the general dimensionless correlation

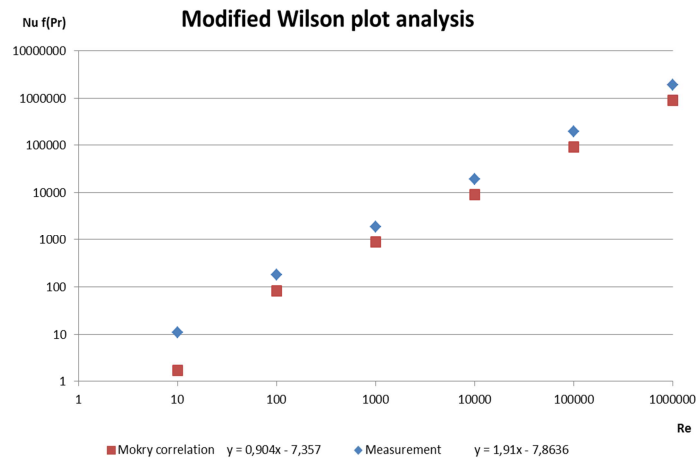


Figure 8. Logarithmic graph describing the Nu number as a function of the Re and Pr numbers (comparison of calculations with measured data)

$Nu = CRe^mPr^n$  are also obtained, thus the general correlation is determined assuming only the value of the exponent of the Prandtl number, n.

$$Nu = 0,0044Re^{1,91}Pr^{0,4} \quad (19)$$

In the design process of this supercritical heat exchanger, three calculation methods for supercritical heat transfer were implemented and compared (Petukhov, Garimella, and Mokry). These heat transfer correlations were developed independently. A safety factor was implanted to account for heat transfer correlation uncertainty. The measurements and the new correlation derived from this experiment indicate (Figure 8) that the measured heat transfer is about 10% higher than the used correlations. Hence, the size of the heat exchanger can be reduced by 10% by keeping the good performance (heat transfer rate). On the other hand, by reducing the size the cost for this component will be lowered and that will have economic benefit on the whole plant as well. As conclusion that can be drawn from this analysis is that by reducing the uncertainty, these heat exchangers can be designed and built with lower safety factor. The benefit would be more accurate design and use of less material which leads to lower costs and lower pressure drop for both fluid circuits.

## 5. CONCLUSIONS

In this work a supercritical heat exchanger suitable for ORC applications is investigated. Even though ORC is not new technology, there is still room for improvement by working at supercritical state of the organic fluid. However, there is still lack of experimental (accurate) data, especially suitable for ORC installations. A helical coil heat exchanger was designed and built. Correlations available from literature were used. These correlations were developed for water, CO<sub>2</sub> and refrigerants like R404a and R410a. The correlations were derived for smaller diameter and different working conditions than ORCs. In order to check the performance at supercritical working conditions set of measurements was conducted. The inlet temperatures of the working and heating fluid were held constant 36,3°C and 101°C respectively. For this measurement the mass flow rate was 0,226 kg/s and the heat exchanger showed good performance. The pinch point temperature difference at these working conditions is lower than 10K. From the mentioned arguments in this paper, it can be concluded that more accurate design of the heat exchanger with appropriate correlations leads to improved cycle efficiency and lowering the cost of such installation. Therefore, this technology can be a promise within the current energy markets.

## 6. REFERENCES

1. Shitsman, M.E., *Heat transfer to water, oxygen and carbon dioxide in the approximately critical range*. Teploenergetiky, No.1, 1959: p. pp.68-72.
2. Dickinson, N.L. and C.P. Weich, *Heat transfer to supercritical water*. ASME 80, 1958: p. pp.745-751.

3. Krasnoshchekov, E.A. and V.S. Protopopov, *Heat transfer at supercritical region in flow of carbon dioxide and water in tubes, (In Russian)*. Thermal Eng., 1959. **12**: p. 26–30.
4. Yamagata, K., et al., *Forced convection heat transfer to supercritical water flowing in tubes* International Journal of Heat and Mass Transfer., 1972. **15**: p. pp.2575-2593.
5. Ackermann, J.W., *Pseudo-boiling heat transfer to supercritical pressure water in smooth and ribbed tubes*. Journal of Heat transfer, 1970. **Vol. (1970)**: p. pp.490-498.
6. Bishop, A.A., R.O. Sandberg, and L.S. Tong, *Forced convection heat transfer to water at near critical temperatures and supercritical pressures*., WCAP-2056-P, Part-III-B, 1964(February, 1964. ).
7. Shitsman, M.E., *Impairment of the heat transmission at super-critical pressures*. . Teplofiz. Vys. Temp. 1, 1963. **No. 2** (1963).
8. Jackson, J.D. and J. Fewster, *Forced Convection Data for Supercritical Pressure Fluids*. HTFS 21540, 1975.
9. Jackson, J.D. and W.B. Hall, *Influences of buoyancy on heat transfer to fluids flowing in vertical tubes under turbulent conditions*. Turbulent Forced Convection in Channels and Rod Bundles, 1979. **2**(published by Hemisphere Publishing Corporat.): p. 613-640.
10. Haskins, H.J., R.M. Taylor, and D.B. Osborn, *Development of solar receiver for an organic Rankine cycle engine*, in *Proceedings of the 16th Intersociety Energy Conversion Engineering Conference. 'Technologies for the Transition'*, 1981. p. 1764-9, vol.2.
11. Lazova M., K.A., Huisseune H., and De Paepe M., *Heat transfer in horizontal tubes at supercritical pressures for ORC application*, in *HEFAT 2014*, 2014.
12. Zhang C-L, Y.L., Shao L-L. , *Comparison of heat pump performance using fin-and-tube and microchannel heat exchangers under frost conditions*. , in *Appl Energy*, 2010. p. 1187–97.
13. Cayer E, G.N., Nesreddine H. , *Parametric study and optimization of a transcritical power cycle using a low temperature source*. , in *Appl Energy* 2010. p. 1349-57.
14. Roy P, D.M., Galanis N, Nesreddine H, Cayer E. , *Thermodynamic analysis of a power cycle using a low-temperature source and a binary NH<sub>3</sub>–H<sub>2</sub>O mixture as working fluid*. . Int J Thermal Sci 2010. **49(1)**: p. 48–58.
15. Claesson, J., *Correction of logarithmic mean temperature difference in a compact brazed plate evaporator assuming heat flux governed flow boiling heat transfer coefficient*. . Int J Refrig, 2005. **28(4)**: p. 573–78.
16. Coates J, P.B., *Heat Transfer to Moving Fluids*, in *Chem Eng* 1959. p. 67–72.
17. Kern, D.Q., *Process Heat Transfer*. , 1950.: McGraw-Hill, New York.
18. Petukhov BS, K.E., Protopopov VS. , *An investigation of heat transfer to fluids flowing in pipes under supercritical conditions*., in *ASME* 1961: University of Colorado, Boulder, CO, USA. p. 569-78.
19. Kakaç S, L.H., Pramuanjaroenkij A. , *Heat exchangers, Selection, Rating, and Thermal design*. , 2012: CRC Press p. 117-118.
20. Petukhov BS, K.V., *On heat exchange at turbulent flow of liquid in pipes*. Teploenergetika 1, 1958. **4**: p. 63–81.
21. Garimella, S., *High condensing temperature heat transfer performance of low critical temperature refrigerants*, 2006, Air-conditioning and refrigeration technology institute, ARTI 21CR program contract number 610-20060, : Arlington, Virginia, USA.
22. Mokry S, P.I., *Development of supercritical water heat-transfer correlation for vertical bare tubes*. , in *Nuclear Engineering and Design*, 2011. p. 1126–1136.
23. Shah, R.K., *Assesment of modified Wilson plot techniques used for obtaining heat exchanger design data in Heat Transfer*, in *9th International heat transfer Conference* 1990. p. 51-56.
24. Jose Fernandez-Seara, J.S.a.A.C., *Experimental apparatus for measuring heat transfer coefficients by the Wilson plot method*. European Journal of Physics 2005.